

## Chapter 14

# Role of Specific Intermolecular Interactions in Modulating Spectroscopic Properties of Photoreactive Compounds Bound to Proteins

Marshall G. Cory, Jr., Nigel G. J. Richards, and Michael C. Zerner

Department of Chemistry, University of Florida, Gainesville, FL 32611

The rational design of photosubstrates will require a detailed understanding of the effects of protein environments upon the spectroscopic properties of small molecule ligands. We here describe preliminary INDO/S calculations upon two models of the complex between a tripeptide containing a 3-amino-isochromene moiety which represents a potential photocaged amide, and the aspartic proteinase, rhizopuspepsin. Hydrogen bonding interactions appear to play an important role in causing a hypochromic (red) shift of approximately 19 nm ( $1800\text{ cm}^{-1}$ ) in the electronic absorption spectrum of the tripeptide chromophore, a substantial difference compared to the absorption maximum associated with the  $n \rightarrow \pi^*$  transition of the tripeptide in the gas-phase. In addition, these calculations confirm that charged groups within the protein are likely to modulate low-energy electronic transitions in the photosubstrate. Our results demonstrate that when computational methods are used to predict the spectroscopic and photochemical reactivity of photocaged compounds, specific interactions between the protein environment and the photosubstrate, such as hydrogen bonds, must be included in the calculation.

The demonstration that synchrotron X-ray sources allow sufficiently rapid data collection for protein crystallography has opened the possibility of directly observing the structural features of enzymes as they catalyze reactions in the solid state (1). For example, interpretable electron density maps at atomic resolution have been obtained for the enzyme glycogen phosphorylase by exposing the crystal to an X-ray beam for only 0.8 second (2). With the solution of the technical problems in data collection, the initiation of reaction in all of the molecules in the crystal at a well-defined instant has become a major hurdle to obtaining snapshots of enzyme-substrate complexes at various stages of reaction (3). For simple reactions, experimental strategies involving either rapid jumps in temperature (4) or pH (5) have been reported as a means for achieving temporal synchronization of reactions throughout the crystal. Indeed, for the enzyme trypsin, identification of the water molecule involved in acylenzyme hydrolysis was achieved using a pH jump to initiate reaction (6) although the detailed interpretation of this experiment remains the subject of some debate (7). An alternative approach has been to obtain compounds which represent caged substrates (often termed "photosubstrates") for the reaction of interest (8), or photolabile enzyme derivatives (9,

0097-6156/94/0569-0222\$08.00/0  
© 1994 American Chemical Society

10) which can be released through the absorption of high-intensity light. Such compounds allow the solution of two problems associated with time-resolved X-ray crystallography (11). First, the unreactive form of the photosubstrate can be designed to possess high affinity for the enzyme active site, resulting in a large occupancy ratio in crystals of the photosubstrate/enzyme complex. Second, photochemical release of the necessary functional group means that reaction is initiated in all of the protein molecules within a narrow time range, leading to coherence in the chemical reactions occurring in every complex in the crystal. Such a temporal coherence potentially allows the detection of long-lived reaction intermediates and/or the complex between protein and reaction products. While the use of 'caged' enzymes in time-resolved X-ray crystallography has not yet yielded data of sufficient quality to be useful (12), the successful use of photosubstrates in allowing direct observation of the complex between Ha-ras p21 protein and GTP has been reported (13).

The development and application of further examples of photosubstrates to study enzyme-catalyzed reactions involving more complex functional groups might be aided by the use of computational strategies for the evaluation of candidate structures. There are a number of stringent design criteria which must be satisfied by such compounds (14). First, any photosubstrate must be closely related, in terms of its gross molecular structure, to the natural substrate so that it has a high affinity for the enzyme active site. Second, the photosubstrate must possess sufficient functionality that the "caged" portion is located correctly within the active site. The photosubstrate must also absorb light at a wavelength at which the protein, the surrounding solvent molecules in the crystal, and the photoproduct are transparent. Finally, the photochemical reaction to unmask the functional group of interest should proceed, in reasonable quantum yield, from the  $S_1$  state to avoid the formation of long-lived radical intermediates which might undergo alternative reactions with the functional groups in the protein.

The inclusion of environment-dependent effects remains a problem of interest in theoretical calculations (15). While efforts in this area have focussed upon the influence of environment on structural preferences and energetics (16, 17), the modulation of photochemical and spectroscopic properties of ligands by their environment remains much less explored (18-20). INDO/S semi-empirical techniques (21-23) have been used successfully to study the spectroscopy of a large number of compounds, including, most recently, the photochemical properties of chlorophyll in the photosynthetic reaction center (24, 25). In this paper we outline the results of preliminary INDO/S calculations on model complexes between a potential photocaged tripeptide incorporating a 3-amino-isochromene moiety and the aspartic proteinase, rhizopuspepsin (26). These studies support the hypothesis that specific, intermolecular hydrogen bonding interactions will be important in modulating the absorption properties of this ligand when bound within the protein.

### **Isochromenes as Potential Photocaged Amides**

Aspartic proteinases represent a particularly important class of enzymes (27) which catalyze the hydrolysis of amide bonds. Many of this family of proteases are involved in critical biological roles, including viral assembly (28) and the regulation of blood pressure (29). Significantly, it is thought that protein loops fold onto the peptide substrate and play a role in mediating catalysis. Support for such a hypothesis has been obtained by site-specific mutagenesis of conserved residues within these regions which affected the rate of the hydrolysis reaction in the mutant enzymes (30). The development of photocaged amides allowing the detailed study of the conformational changes occurring within these loops during catalysis might therefore provide new insight into their functional role. We have recently proposed that 3-amino-

isochromenes, of general structure 1, might represent photocaged amides (Figure 1) (31) since irradiation of such compounds should effect an electrocyclic reaction to generate an amide bond. Trapping of the reactive intermediate 2 by a water molecule should then yield a stable substrate which can be hydrolyzed by the aspartic proteinase. Our hypothesis is preceded by studies upon the photochemical reactivity of 3-phenyl-isochromenes in which the existence of such a ring-opened intermediate was demonstrated experimentally (32, 33). We have also shown that INDO/S calculations can reliably reproduce the spectroscopic and photochemical behavior observed experimentally for this class of compounds (31). These previous calculations employing a self-consistent reaction field (SCRF) (20, 34-37) to represent solvent, indicated that the inclusion of explicit hydrogen bonds between solvent and the oxygen atom of the isochromene chromophore was necessary to calculate the UV-visible absorption bands correctly (31). The requirement that specific interactions must be included in an SCRF model is not too surprising (36, 37). At the SCF level, the reaction field stabilizes the ground state of a molecule through its response to any asymmetric distribution of charge, by an amount  $\Delta E_0$  given, at the dipolar level, by:

$$\Delta E_0 = - [ g(\epsilon) \cdot \mu_0 >^2 ] / 2$$

where  $g(\epsilon)$  is the Onsager reaction factor (37),  $\epsilon$  is the dielectric constant of the solvent and  $\mu_0$  is the dipole moment of the ground state structure. In the case of an amino-isochromene, this term would correspond to a dipole-image dipole interaction. Such a description is incomplete when solvent molecules can interact by hydrogen bonding. Not only is the dipole moment associated with the ground state of the molecule diminished, but the orbital energies are also specifically affected by the solvent. Hydrogen-bond interactions must therefore be explicitly introduced into the model through the use of a super-molecule, and it is the optimized ground state structure of the super-molecule which must be used to obtain the UV-visible spectrum in the INDO/S-SCRF-CIS calculation (36, 38). Electronic excitation in a molecule occurs in  $10^{-15}$  to  $10^{-18}$  seconds, and solvent nuclei cannot change their positions during the absorption process. However, electronic polarization of the solvent can occur within this timeframe. Inclusion of this effect in the SCRF calculation to first order in perturbation theory (37) yields the following expression (model B in reference 37):

$$\Delta E^*_{abs} = - [ g(\epsilon) \cdot \mu_0 > \cdot \mu_* > ] / 2 + [ g(\eta^2) \cdot \mu_* > \cdot (\mu_0 > - \mu_* >) ] / 2$$

Here,  $\Delta E^*_{abs}$  is change in energy of the excited state of the molecule relative to the gas-phase, immediately after excitation,  $\mu_*$  is the dipole moment of the excited state,  $g(\eta^2)$  is the Onsager reaction factor and  $\eta$  is the refractive index of the solvent. Thus the change in the energy  $\Delta\Delta E$  required for the electronic transition in the SCRF model, relative to that in the gas-phase, is given by:

$$\Delta\Delta E = - [ \{ g(\epsilon) \cdot \mu_0 > + g(\eta^2) \cdot \mu_* > \} \cdot (\mu_0 > - \mu_* >) ] / 2$$

In general, this implies that if the ground state dipole is greater than that of the excited state, the absorption band will be blue-shifted, and vice versa. In the 3-amino-isochromene structure (1, Figure 1) the two lowest lying excitations are  $n \rightarrow \pi^*$ ,

principally from the lone pairs of the nitrogen atom attached to the isochromene moiety to the  $e_g(\pi^*)$  molecular orbitals of the benzene ring. The degeneracy of the  $e_g(\pi^*)$  is split by the presence of the fused heterocyclic ring. Both of these excitations lead to a large change in the electronic distribution in the chromophore, resulting in the dipole moment of the excited state being larger than that of the ground state structure. By itself, this would lead to a red shift of the associated absorption bands, but specific interactions involving the nitrogen lone pair, were they to be present, might also modulate the energy of the electronic excitations. In order to establish the magnitude of such environmental effects in designing photosubstrates, we have investigated the perturbation of the absorption properties of a model peptide incorporating the 3-amino-isochromene moiety when bound to the active site of rhizopuspepsin. Since it was likely that specific hydrogen bonds would be formed between the protein and the heteroatoms in the peptide, we anticipated that there would be significant shifts in the absorption properties of the heterocyclic moiety relative to those in the gas-phase. Tripeptide 3 (Figure 2) was chosen as a model compound for these calculations, as (1) this represented the smallest unit which might be accommodated within the binding pocket of rhizopuspepsin, and (2) the complex between rhizopuspepsin and the inhibitor, 4, which incorporated a similar structural fragment, had been determined crystallographically (39, 40).

### Modeling the Complex between Rhizopuspepsin and the Model Photosubstrate 3

Two initial models of the tripeptide 3 within the proteinase binding pocket were constructed using the X-ray crystal coordinates of the complex between the inhibitor 4 (Figure 2) and rhizopuspepsin (40) obtained from the Brookhaven Protein Database (41) (2APR). These structures, 5 (Figure 3A) and 9 (Figure 3B) differed in the protonation state of Asp-35 as the binding of tripeptide 3 within rhizopuspepsin might alter the pKa of the ionizable, sidechain carboxylic acid group of this residue. Thus, Asp-35 was ionized in 5 and in its neutral form in 9. This catalytically active residue is usually presumed to exist in its protonated form so as to be able to act as a general acid in the initial step of the amide hydrolysis reaction (42). The inhibitor structure 4 was graphically modified so as to yield the tripeptide structure 3 with minimal modification of all rotatable dihedral angles. The all-atom structures ( $\approx 3000$  atoms) of both complexes 5 and 9 were energy minimized using a truncated Newton-Raphson optimization algorithm (43), as implemented in BATCHMIN V3.5 (44), until the total residual RMS gradient, representing the forces on the atoms, was less than 0.01 kJ/Å (45). Both empirical force field calculations employed the OPLSA potential energy function and parameters (46) augmented by the GB/SA continuum solvation potential for water (47). Simulated annealing was then used to ensure that tripeptide 3 was optimally docked into the protein in both models of the peptide/protein complex (48). The INDO/S calculations employed structures which comprised all atoms in the tripeptide 3 together with the atoms in the following residues: Asp-35, Thr-36, Gly-37; Tyr-77, Gly-78; Asp-218, Thr-219, Gly-220, Thr-221. In addition, each of the three protein segments (35-37; 77-78; 218-221) were modeled as their N-terminal amides and C-terminal methylamides. The location of the additional atoms in the terminal amide groups were defined by the coordinates of the carbonyl group and  $C_\alpha$  of the preceding (34, 76 and 217), and the NH and  $C_\alpha$  of the following (37, 79 and 222), residues in the protein structure. Hence, models of a suitable size for the INDO/S calculations ( $\approx 200$  atoms) on the potential photosubstrate 3 when bound to rhizopuspepsin were obtained in which all of the critical intermolecular interactions were present (Figures 3A and 3B). Given the difference in the ionization state of the Asp-35 sidechain in these models, after energy minimization of the complexes,

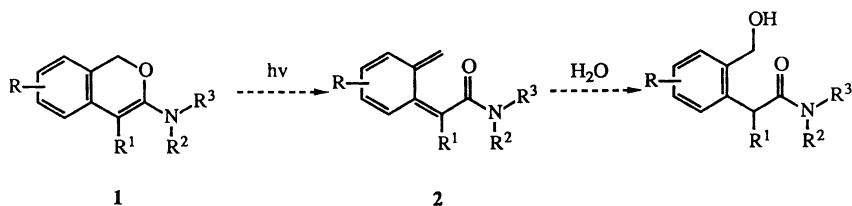


Figure 1. Potential photochemical ring-opening reaction of 3-aminoisochromenes to release a masked amide bond.

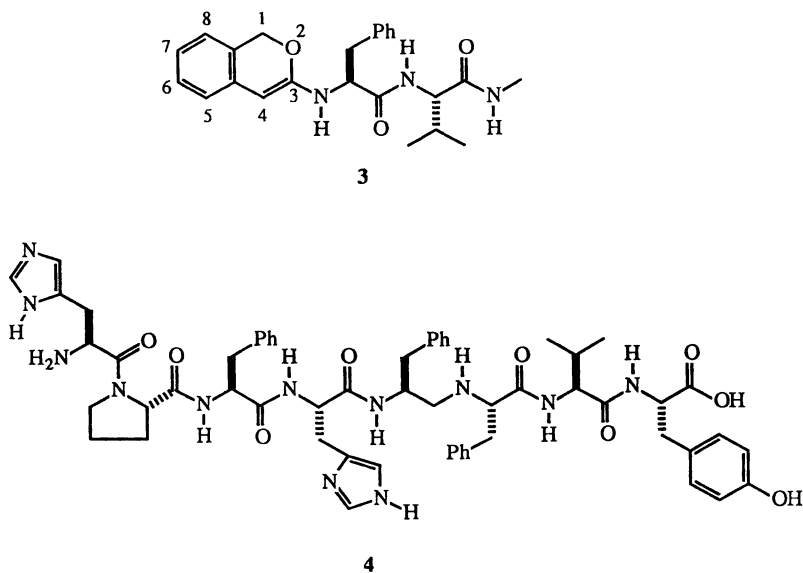


Figure 2. Structures of the tripeptide photosubstrate **3** used in these calculations, and the 'reduced' amide inhibitor **4** used to build the initial model of the complex between **3** and rhizopuspepsin. Small numbers indicate the numbering system for atoms within the isochromene ring.

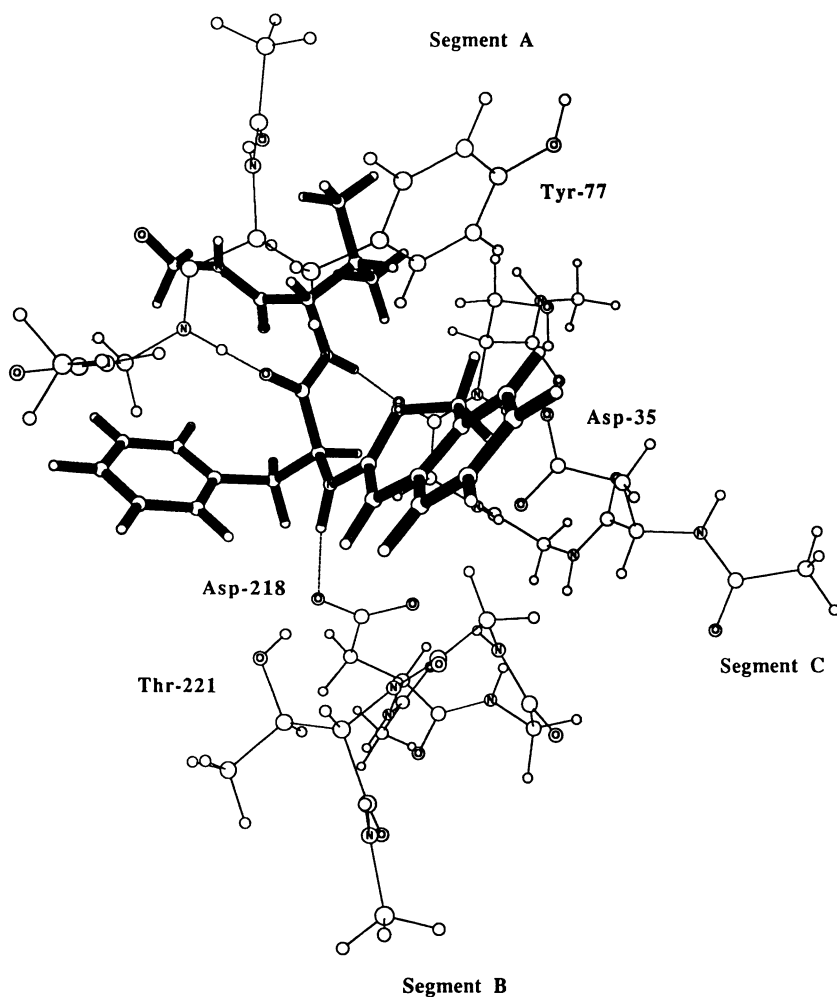


Figure 3. Schematic representations of the subsite models of the complex between tripeptide 3 and the active site residues of rhizopuspepsin. In both figures bonds, intermolecular hydrogen bonding interactions are shown as dotted lines, all bonds in the protein fragments are drawn as single lines irrespective of bond order, and the tripeptide structure is drawn using "thick-lines". Nitrogen and oxygen atoms are represented by the symbols N and O, respectively. (A) Complex 5 in which Asp-35 is in the ionized form.

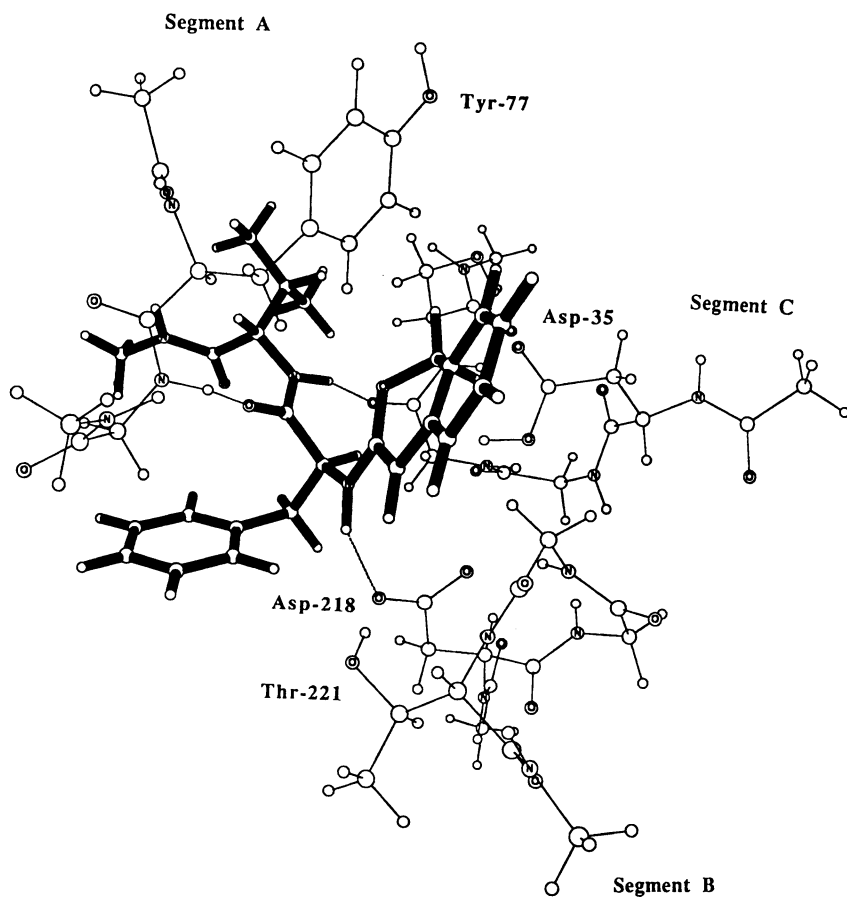


Figure 3. (B) Complex 9 in which Asp-35 is protonated.

tripeptide **3** was bound in two non-identical, although similar, conformations (**3-a** and **3-b**). All subsequent calculations upon the *in vacuo* absorption properties of **3** were therefore carried out upon both **3-a** and **3-b** so that differences in the absorption spectra arising from their specific interactions with the protein were correctly determined.

In the complex **5** in which Asp-35 was modeled as the carboxylate, three hydrogen bonds were detected between the tripeptide in conformation **3-A** and the protein fragments in the optimized structure (Figure 3A). Of particular interest was the hydrogen bond between the NH group of the substituted isochromene and the sidechain of Asp-218, which represented a direct intermolecular interaction that we anticipated would perturb the spectroscopic and photochemical properties of the isochromene group. The aromatic rings of Tyr-77 and the isochromene moiety were in close proximity, raising the possibility that charge transfer between the two  $\pi$ -systems might also be involved in modulating the absorption properties of the isochromene unit when bound to the protein (49). For the complex **9** in which Asp-35 was in its protonated, neutral form (Figure 3B), four hydrogen bonds were present in addition to the potential interaction between the aromatic sidechain of Tyr-77 and the isochromene moiety. While three of the hydrogen bonds in **9** were identical to those in **5**, an additional, weak, hydrogen bond appeared to be present between O-2 in the isochromene unit (Figure 2) and the carboxylic acid group of Asp-35 (Figure 3B).

Our initial INDO/S calculations explored the effects of the protonation state of Asp-35 upon the spectroscopic properties of **3** when bound within the protein. Single-point SCF calculations on the two model structures, **5** and **9**, were carried out using ZINDO (50) executing on an IBM RS/6000 PowerStation Model 580, in order to obtain the molecular orbitals used to construct the spin-adapted many-electron basis. In these, and all subsequent, calculations a minimal basis set was employed representing only the valence orbitals on each atom. Configuration interaction calculations over singly excited configurations (CIS) were then performed to obtain the UV-visible absorption spectra for these model complexes (Tables I and II). *In vacuo* CIS calculations were also performed for the two conformations of the tripeptide (**3-a** and **3-b**) so as to evaluate the change in the spectroscopic properties of isochromene due to specific interactions with the protein (Tables I and II). For the isolated ligand **3-a**, in the conformation present in peptide/protein complex **5**, there was a strong absorption at 312.4 nm corresponding to an  $S_1$  state, comprising 79% of the HOMO $\rightarrow$ LUMO transition (38) and 15% of the HOMO $\rightarrow$ LUMO+3 transition within the MO picture. For **3-b**, the cognate absorption occurred at 313.9 nm. While the difference in energy between these two calculated bands is unimportant, the presence of two low energy bands with significant oscillator strength indicated that the  $S_1$  and  $S_2$  states of the isolated ligand, for both conformations, were close in energy. Variation of the active CIS space, beyond 10-up/10-down, had little effect upon the calculated absorptions or intensities for the model complexes, suggesting that all of the relevant protein and ligand orbitals had been included in our initial computations. This 'control' series of independent CIS calculations employed orbitals from 20-up/20-down to 45-up/45-down centered about the HOMO-LUMO gap. In both model complexes **5** and **9**, the low-energy, electronic transitions cognate to those calculated for the ligand *in vacuo* were shifted to lower energy by about 19 nm (1800  $\text{cm}^{-1}$ ) and 13 nm (1485  $\text{cm}^{-1}$ ) for **3-a** and **3-b**, respectively (Tables I and II). The difference in the magnitude of the red shift also appeared to be related to the ionization state of Asp-35. In the  $S_1$  excited state, **3-a** possesses a large dipole due to transfer of charge from the 3-amino substituent to the benzene ring of the isochromene group. Electrostatic stabilization by the charged sidechain should therefore play a direct role in modulating the isochromene absorption spectrum. While it is possible that the shift also results from modification of the MO energies associated with the  $S_0$  state, no evidence for this was observed in



**Table I** Major absorption bands of tripeptide 3 in a series of models of its complex with rhizopuspepsin

Structure <sup>a</sup> (CI)	State	Absorption $\lambda$ (nm) $\nu$ (1000 cm <sup>-1</sup> )		Oscillator Strength	Atoms	Basis Functions
<b>5</b> (35x35)	S1	331.6	30.2	0.56	200	518
	S2	326.8	30.6	0.04		
	S26	233.1	42.9	0.23 (x)		
	S27	230.7	43.4	0.19 (y)		
<b>6</b> (35x35)	S1	332.1	30.1	0.59	189	486
	S2	327.6	30.5	0.05		
	S17	233.1	42.9	0.25 (x)		
	S19	217.8	45.9	0.09 (y)		
<b>7</b> (20x20)	S1	332.7	30.0	0.63	160	415
	S2	328.8	30.4	0.04		
	S13	227.8	43.9	0.36 (x)		
	S19	217.5	45.9	0.09 (y)		
<b>8</b> (20x20)	S1	327.8	30.5	0.30	111	285
	S2	320.5	31.2	0.39		
	S14	229.6	43.6	0.20 (x)		
	S18	215.0	46.5	0.07 (y)		
<b>3-a</b> (20x20)	S1	312.4	30.5	0.51	59	149
	S2	308.9	31.2	0.13		
	S8	225.8	43.6	0.12		
	S9	224.9	44.5	0.21 (x)		
	S12	213.7	46.8	0.08 (y)		

<sup>a</sup>5; Figure 3A: 6; Figure 3A, Tyr-77 replaced by alanine: 7; Figure 3A minus peptide segment A: 8: Figure 3A minus peptide segments A and C. In all models of the complex, the sidechain of Asp-35 of the protein is modeled as the carboxylate anion. Conformation 3-a is identical to that present in the enzyme-substrate complexes 5-8, and was used to calculate the gas-phase absorption spectrum. The first excited state is always reported. Numbers in brackets refer to the size of the CI (orbitals up/orbitals down). Only those excited states with significant oscillator strength are given subsequently.

**Table II** Major absorption bands of tripeptide **3** in a series of models of its complex with rhizopuspepsin

Structure <sup>a</sup> (CI)	State	Absorption		Oscillator Strength	Atoms	Basis Functions
		$\lambda$ (nm)	$\nu$ (1000 cm <sup>-1</sup> )			
<b>9</b> (35x35)	S1	327.6	30.5	0.36	201	519
	S2	319.2	31.3	0.27		
	S24	230.8	43.3	0.22 (x)		
	S25	229.6	43.6	0.11 (y)		
<b>10</b> (35x35)	S1	327.3	30.5	0.36	190	487
	S2	319.3	31.3	0.33		
	S20	225.9	44.3	0.29 (x)		
	S24	215.7	46.4	0.08 (y)		
<b>11</b> (20x20)	S1	328.7	30.4	0.32	161	416
	S2	325.9	30.7	0.03		
	S3	320.7	31.2	0.36		
	S14	225.9	44.3	0.30 (x)		
	S19	216.8	46.1	0.08 (y)		
<b>12</b> (20x20)	S1	327.5	30.5	0.30	112	286
	S2	320.2	31.2	0.39		
	S14	229.2	43.6	0.21 (x)		
	S18	214.8	46.5	0.07 (y)		
<b>3-b</b> (20x20)	S1	313.9	31.9	0.54	60	150
	S2	309.9	32.3	0.11		
	S9	225.5	44.3	0.30 (x)		
	S12	213.8	46.8	0.08 (y)		

<sup>a</sup>**9**; Figure 3B: **10**; Figure 3B, Tyr-77 replaced by alanine: **11**; Figure 3B minus peptide segment A: **12**; Figure 3B minus peptide segments A and C. In all models of the complex, the sidechain of Asp-35 of the protein is modeled as the as the neutral, carboxylic acid. Conformation 3-b is identical to that present in the enzyme-substrate complexes **9-12**, and was used to calculate the gas-phase absorption spectrum. The first excited state is always reported. Numbers in brackets refer to the size of the CI (orbitals up/orbitals down). Only those excited states with significant oscillator strength are given subsequently.

these calculations. Visualization of the molecular orbitals involved in these electronic transitions (51) indicated that the excitation was exclusively located on the isochromene moiety of 3, and probably corresponded to that already shown to be involved in the desired ring-opening reaction for 3-phenylisochromenes (31). The energy splitting of these two states also appeared sensitive to the protein environment. For the two ligand conformations, 3-a and 3-b, in the gas-phase,  $S_1$  and  $S_2$  were split by 400  $\text{cm}^{-1}$ , while the energy splitting in 5 was smaller than in 9 (400  $\text{cm}^{-1}$  and 800  $\text{cm}^{-1}$ , respectively). Equally, the partitioning of oscillator strength between  $S_1$  and  $S_2$  was affected by the presence of the protein. For both conformations of the isolated ligand, the ratio of the oscillator strengths was about 4:1. On the other hand, although in both 5 and 9, the oscillator strengths of  $S_1$  and  $S_2$  summed to approximately 0.65, our calculations indicated that the low-energy region of the absorption spectrum of the 3-amino-isochromene in complex 5 should only consist of comprise a single peak. This contrasts with the case of 9 which consists of two peaks of equal intensity. These results suggest that it might be possible to use the electronic absorption properties of bound ligands to distinguish between the ionization states of groups within proteins.

### Modulation of Absorption by Specific Intermolecular Interactions

We reasoned that the stabilization of the  $S_1$  excited state of the isochromene was principally due to the hydrogen bonding interactions with the protein and therefore carried out some simple calculations to determine if this hypothesis was qualitatively correct. For each subsite model of the complex between rhizopuspepsin and tripeptide 3 we therefore explored the effects of specific protein-ligand interactions in contributing to the large shift in the lowest energy absorption band from its gas-phase value (Tables I and II). To do this, a series of model complexes were constructed by the systematic removal of protein fragments participating in specific intermolecular interactions with the tripeptide 3, and their electronic spectra calculated. Hence, complex 6 was obtained from 5 by removal of the aromatic sidechain of Tyr-77 so as to generate an alanine residue (Figure 3A). In turn, complexes 7 and 8 were obtained by deletion of the peptide fragments corresponding to segments 77-87 (Segment A in Figures 3A and 3B) and 218-221, respectively (Segment C in Figures 3A and 3B). Complexes 10-12 were obtained by an identical procedure to that used for 6-8 except that complex 9, in which Asp-35 was protonated, was used as the starting structure. For all complexes, the only significant modifications to the spectroscopic properties of 3 occurred when the hydrogen bonding interaction between the NH-substituent on the isochromene and the carboxylate of Asp-218 was broken. This accords with our previous observations upon the importance of modeling specific hydrogen bonding interactions in calculating the properties of heterocyclic chromophores (31). We also note that in every system there are two relatively strong bands that we designate (x) and (y) (Tables I and II) which are probably associated with the 3-amino-isochromene chromophore. However, tripeptide conformation 3-a possesses an additional band arising from the  $S_8$  state which has little intensity in any of the complexes and in 3-b. Thus, more subtle effects due to chromophore conformation and to the protein environment may be operating. Equally, the importance of dynamic effects has not been evaluated in this study, and more sophisticated calculations employing 'snapshots' from QM/MM simulations (16) of peptide/protein complexes will probably be required to address this issue.

### Conclusions

While providing only a qualitative picture of the effect of protein environment on the absorption properties of small molecules, these calculations reveal the importance of

specific hydrogen bonding interactions in causing significant shifts in absorption bands in the UV-visible region. We therefore conclude that rational discovery of novel photocaged compounds using computational approaches must include such interactions specifically within the model. Current efforts are centered upon the synthesis and characterization of peptides containing the isochromene moiety to verify the results of our calculations. The outcome of these studies will be reported in due course.

### Acknowledgments

Partial funding for this work was provided through a Research Development Award from the Division of Sponsored Research at the University of Florida, Proctor and Gamble, and CAChe Scientific, Inc. (NGJR). This work was also supported in part by the Office of Naval Research (MGC, MCZ).

### Literature Cited

- Hajdu, J.; Johnson, L.N. *Biochemistry* **1990**, *29*, 1669.
- Moffat, K. *Annu. Rev. Biophys. Biophys. Chem.* **1989**, *18*, 309.
- Hajdu, J.; Acharya, K. R.; Stuart, D. I.; McLaughlin, P. J.; Barford, D.; Oikonomarkos, N. G.; Klein, H.; Johnson, L. N. *EMBO J.* **1987**, *6*, 539.
- Ringe, D.; Stoddard, B. L.; Bruhnke, J.; Koenigs, P.; Porter, N. *Phil. Trans. R. Soc. Lond. [A]* **1992**, *340*, 273.
- Rasmussen, B. F.; Stock, A. M.; Ringe, D.; Petsko, G. A. *Nature(Lond.)* **1992**, *357*, 423.
- Pai, E. F.; Schulz, G. E. *J. Biol. Chem.* **1983**, *258*, 1752.
- Singer, P. T.; Smalås, A.; Carty, R. P.; Mangel, W. F.; Sweet, R. M. *Science* **1993**, *259*, 669.
- Perona, J. J.; Craik, C. S.; Fletterick, R. J. *Science*, **1993**, *261*, 620.
- McCray, J. A.; Trentham, D. R. *Annu. Rev. Biophys. Biophys. Chem.* **1989**, *18*, 239.
- Stoddard, B. L.; Koenigs, P.; Porter, N.; Petratos, K.; Petsko, G. A.; Ringe, D. *Proc. natl. Acad. Sci., U. S. A.* **1991**, *88*, 5503.
- Mendel, D.; Ellman, J. A.; Schultz, P. G. *J. Am. Chem. Soc.* **1991**, *113*, 2758.
- Moffat, K.; Chen, Y.; Ng, K.; McRee, D.; Getzoff, E. D. *Phil. Trans. R. Soc. Lond. [A]* **1992**, *340*, 175.
- Stoddard, B. L.; Bruhnke, J.; Koenigs, P.; Porter, N.; Ringe, D.; Petsko, G. A. *Biochemistry* **1990**, *29*, 8042.
- Schlichtling, I.; Almo, S. C.; Rapp, G.; Wilson, K.; Petratos, K.; Lentfer, A.; Wittinghofer, A.; Kabsch, W.; Pai, E. F.; Petsko, G. A.; Goody, R. S. *Nature(Lond.)* **1990**, *345*, 309.
- Corrie, J. E. T.; Katayama, Y.; Reid, G. P.; Anson, M.; Trentham, D. R. *Phil. Trans. R. Soc. Lond. [A]* **1992**, *340*, 233.
- Field, M. J.; Bash, P. A.; Karplus, M. *J. Comput. Chem.* **1990**, *11*, 700.
- Cramer, C. J.; Truhlar, D. G. *J. Am. Chem. Soc.* **1991**, *113*, 8305.
- Wong, M. W.; Wiberg, K. B.; Frisch, M. J. *J. Am. Chem. Soc.* **1992**, *114*, 1645.
- Luzkhov, V.; Warshel, A. *J. Am. Chem. Soc.* **1991**, *113*, 4491.
- Rauhut, G.; Clark, T.; Steinke, T. *J. Am. Chem. Soc.* **1993**, *115*, 9174.
- Ridley, J. E.; Zerner, M. C. *Theoret. Chim. Acta* **1973**, *32*, 111.
- Ridley, J. E.; Zerner, M. C. *J. Mol. Spectrosc.* **1974**, *50*, 457.
- Pople, J. A.; Beveridge, D.; Dobosh, P. A. *J. Chem. Phys.* **1967**, *47*, 2026.
- Thompson, M. A.; Zerner, M. C. *J. Am. Chem. Soc.* **1991**, *113*, 8210.

25. Thompson, M. A.; Zerner, M. C. *J. Am. Chem. Soc.* **1990**, *112*, 7828.
26. Chen, Z.; Han, H. P.; Wang, X. J.; Koelsch, G.; Lin, X. L.; Hartsuck, J. A.; Tang, J. *J. Biol. Chem.* **1991**, *266*, 11718.
27. *Structure and Function of Aspartic Proteinases*; Dunn, B. M., Ed.; Advances in Experimental Biology 306; Plenum Press: New York, NY, 1992.
28. Kohl, N. E.; Emmini, E. A.; Schleif, W. A.; Davis, L. J.; Heimbach, J. C.; Dixon, R. A. F.; Scolnik, E. M.; Sigal, I. S. *Proc. natl. Acad. Sci., U. S. A.* **1988**, *85*, 4686.
29. Sielecki, A. R.; Hayakawa, K.; Fujinaga, M.; Murphy, M. E. P.; Fraser, M.; Muir, A. K.; Carilli, C. T.; Lewicki, J. A.; Baxter, J. D.; James, M. N. G. *Science* **1989**, *247*, 454.
30. Suzuki, J.; Sasaki, K.; Sasao, Y.; Hamu, A.; Kawasaki, H.; Nishiyama, M.; Horinouchi, S.; Beppu, T. *Prot. Eng.* **1989**, *2*, 563.
31. Richards, N. G. J.; Cory, M. G., Jr. *Int. J. Quantum Chem., Quant. Biol. Symp.* **1992**, *19*, 65.
32. Padwa, A.; Au, A.; Lee, G. A.; Owens, W. J. *Org. Chem.* **1975**, *40*, 1142.
33. Padwa, A.; Au, A.; Owens, W. J. *Chem. Soc. Chem. Commun.* **1974**, 675.
34. Tapia, O.; Goscinski, O. *Mol. Phys.* **1975**, *29*, 1653.
35. Karelson, M. M.; Katritzky, A. R.; Szafran, M.; Zerner, M. C. *J. C. S. Perkin Trans. 2* **1990**, 195.
36. Karelson, M. M.; Zerner, M. C. *J. Am. Chem. Soc.* **1990**, *112*, 9405.
37. Karelson, M. M.; Zerner, M. C. *J. Phys. Chem.* **1992**, *96*, 6949.
38. Abbreviations used in this paper include: SCF, self-consistent field; CIS, configuration interaction single excitations; SCRF, self-consistent reaction field; HOMO, highest occupied molecular orbital; LUMO, lowest unoccupied molecular orbital.
39. Davies, D. R. *Annu. Rev. Biophys. Biophys. Chem.* **1990**, *19*, 189.
40. Suguna, K.; Padlan, E. A.; Smith, C. W.; Carlson, W. D.; Davies, D. R. *Proc. natl. Acad. Sci., U. S. A.* **1977**, *74*, 7009.
41. Bernstein, F. C.; Koetzle, T. F.; Williams, G. J. B.; Meyer, E. F. Brice, M. D.; Rodgers, J. R.; Kennard, O.; Shimanouchi, T.; Tasumi, M.; *J. Mol. Biol.* **1977**, *112*, 535.
42. James, M. N. G.; Sielecki, A. R.; Hayakawa, K.; Gelb, M. H. *Biochemistry* **1992**, *31*, 3872.
43. Schlick, T.; Overton, M. J. *Comput. Chem.* **1987**, *8*, 1025.
44. Mohamadi, F. M.; Richards, N. G. J.; Guida, W. C.; Liskamp, R. M. J.; Lipton, M. A.; Caufield, C. E.; Chang, G.; Hendrickson, T. F.; Still, W. C. *J. Comput. Chem.* **1990**, *11*, 440.
45. White, D. N. J. *Comput. Chem.* **1977**, *1*, 225.
46. Jorgenson, W. L.; Tirado-Rives, J. *J. Am. Chem. Soc.* **1988**, *110*, 1657.
47. Still, W. C.; Tempczyk, A.; Hawley, R. C.; Hendrickson, T. F. *J. Am. Chem. Soc.* **1990**, *112*, 6127.
48. Kirkpatrick, S.; Gelatti, C. D. J.; Vecchi, M. P. *Science*, **1983**, *220*, 671.
49. *Photophysics of Aromatic Molecules*; Birks, J. B.; Wiley-Interscience: London, 1970; p. 489.
50. ZINDO, a semi-empirical package written by M. C. Zerner and colleagues, University of Florida.
51. Purvis, G. D., III. *J. Comput.-Aided Mol. Des.* **1991**, *5*, 55.

RECEIVED June 2, 1994